HOLOGRAPHIC EVALUATION OF THE HEAT TRANSFER COEFFICIENT ON SUBCOOLED DROPLETS INJECTED INTO A CONDENSABLE ENVIRONMENT

A. CHAVEZ, F. MAYINGER*

Instituto de Investigaciones Eléctricas, FE, Sistemas de Combustión
Apartado Postal 475, 62000 Cuernavaca, Mor. México, Fax: (73) 18 98 54
* Lehrstuhl A für Thermodynamik, Technische Universität München
Arcisstr. 21, 8000 München 2, F.R. Germany

ABSTRACT

Results of the application of holographic methods for direct measurement of the growth of subcooled spray droplets in a pure saturated vapour and evaluation of the direct-contact condensation are presented. The spray flow of the model fluid, refrigerant R113 (trifluorotrichloroethane), is formed by injecting it through a 60° pressure-swirl nozzle of 0.6 mm in bore diameter into its own saturated vapour. The spray flow corresponds to droplet Reynolds numbers in the range $100 \leq Re \leq 3500$ while the vapour pressure is varied in a wide range of reduced pressures $(0.03 \leq p_r \leq 0.3)$.

1. INTRODUCTION

Direct measurements of the heat transfer coefficient at the phase interface between droplets and a continuous vapour phase are of interest for many processes of the energy and chemical industries (i.e. cooling of the nuclear reactor core at LOCA situations, attemperation of superheated steam, direct-contact condensation, drying and humidifying processes, etc.). There is a large series of correlations in the literature which attempt to predict the heat transfer coefficient at a droplet. Most of them base upon the rigid sphere assumption as quoted by **Lautenschlager (1988)**. The general form of these correlations is

$$h_D = \frac{\lambda_v}{D}\left[2 + a\, Re_D{}^b\, Pr_l{}^c\right] \qquad (1)$$

where h_D means the heat transfer coefficient at the droplet, D represents the droplet diameter, a, b and c are constants to be fitted, Re_D means the droplet Reynolds number and Pr_l the Prandtl number of the liquid phase. In this work, the droplet Reynolds number is defined as

$$Re_D = \frac{\varrho_v\, U\, D}{\eta_v} \qquad (2)$$

with U meaning the droplet velocity relative to the vapour phase and ϱ_v and η_v the density and viscosity of the vapour respectively. If $U = 0$ Eq.(1) reduces to the known equation of heat diffusion from a sphere

$$h_D = 2\,\frac{\lambda_v}{D} \qquad (3)$$

where λ_v means the thermal conductivity of the vapour phase.

Sideman & Shabatai (1964) estimated an increase of the heat transfer coefficient around a factor of $1.9\,(Pr_l)^{\frac{1}{6}}$, if an internal circulation in the droplets is assumed. This means an increase of about 3 or 4 times the values calculated with correlations of the form of Eq.(2). At the same time **Hasson, et al. (1964)** reported measurements of the heat transfer coefficient on water sheets arising values of about 100 kW/m^2 K, which agree with the estimation by Sideman and Shabatai.

In a comprehensive literature review **Chávez (1991)** remarks the lack of experimental evidence with respect to local measurements at droplets and emphasizes the necessity to obtain experimental data, in order to validate numerical solutions used for equipment and process design.

This article presents the results of applying holographic methods for direct measurement of the size and growth of subcooled spray droplets in a pure saturated vapour. From these measurements it was possible to calculate the total energy absorbed by the droplets during the time they move through the vapor environment and to perform an evaluation of the heat transfer coefficient. The spray flow of the model fluid, refrigerant R113 (trifluorotrichloroethane), is formed by injecting it through a 60°pressure-swirl nozzle of 0.6 mm in bore diameter into its own saturated vapour. The spray flow corresponds to droplet Reynolds numbers in the range $100 \leq Re_D \leq 3500$ while the vapour pressure is varied in a wide range of reduced pressures $(0.03 \leq p_r \leq 0.3)$.

2. SCOPE OF THE WORK

The emphasis of the present work is dedicated to explain the method which we applied to measure the growth of spray droplets when saturated vapour is condensing on them. Based upon these measurements, calculations

of the condensation rate and of the heat transfer coefficient are presented. For the droplet growth evaluation, we assume that a set of clear single and double pulsed holograms of the spray at steady state conditions can be obtained for dropsizing and drop velocity measurements respectively (for details on the holographic method see Chávez & Mayinger, 1988). We also assume that it is possible to perform detailed evaluations of the holograms; specially of the droplet zone of the spray by applying digital image processing as presented by Chávez & Mayinger (1989).

Table 1 resumes the spray flow conditions at which the holograms were recorded. Here, each "x" corresponds to 4 holograms; two single and two double pulsed holograms, in each case, once taken in the nozzle near region and the other one in the far region with respect to the nozzle. The capitals A to E and the numbers 1 to 8, which are related to the mass flow rate and vapour pressure respectively, are used to distinguish the holograms as A1, A2,... E1, E8. Besides, the letters "n" (nozzle near region) and "f" (far region) are added to complete the code of each hologram (i.e. A1n, A1f, etc.).

3. MEASURING METHOD FOR SIZE AND VELOCITY OF THE SPRAY DROPLETS

As mentioned earlier, the off-axis pulsed laser holography was used as a measuring method. It allows to record a scene of the spray in a very short time (30 ns) which can be reconstructed later for detailed studies and evaluation. In the reconstructed scene, the spray appears as a set of static droplets as if they would be suspended in the air, which can be observed directly as a conventional hologram or with the aid of a videocamera. By applying this last alternative, we can take advantage of digital image processing techniques for droplet measuring and classifying. An example of the appearence of the spray observed by the videocamera from a holographic reconstruction is presented in Fig.1. Here, the photographs **A** to **D** show the focussing process. The nozzle is included for better orientation. **A** represents an original view and **B** to **D** successive filtering operations of **A** leading to a representation (**D**), which can be easily identified by the measuring algorithms. An enlargement **A1** of the droplet zone of picture **A** is shown to illustrate the process of noise filtering (**A2** to **A4**) and the final result in **A4**. With the aid of this procedure, we obtain dropsize distributions and the positions of the droplets in the view field of the hologram.

Complementarily, the drop velocities can be measured by applying double pulsed laser holography. In this case, the holograms represent a conglomeration of spot couples, in which each couple means a spray droplet imaged at two successive positions corresponding to the times $t = t_1$ and $t = t_2$, where $t_2 - t_1 = \Delta t$ is the time intervall between the two exposures used to take the hologram. Δt can be adjusted between 1 - 800 μs in order to facilitate the evaluation in the holographic view field. This kind of hologram presents a strong loss in resolution and therefore, they cannot be used to measure the dropsize. In spite of that, the centroids of the droplet images can be easily recognized to measure the distance between them.

Table 1. Experimental Matrix

$\dot{M}$ (g/s)	p_v MPa								
	0,10	0,15	0,20	0,25	0,40	0,60	0,80	1,00	
0,80	x	x	x	x	x	x	x	x	A
1,37	x	x	x	x	x	x	x	x	B
2,00	x	x	x	x	x	x	x	x	C
2,72	x	x	x	x	x	x	x	x	D
3,86	x	x	x	x	x	x	x	x	E
	1	2	3	4	5	6	7	8	

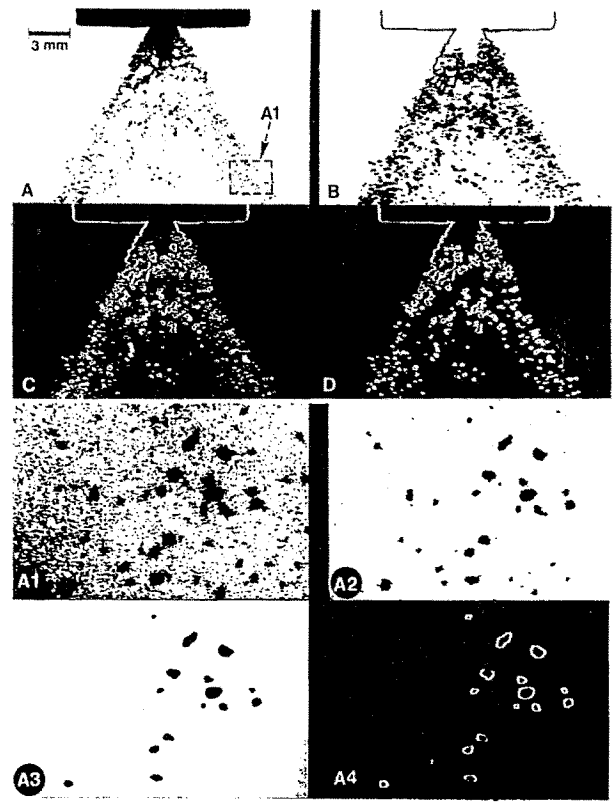

Fig. 1. Representative steps of the image processing of a single pulsed hologram of the R113 spray.
(A) Original image, (B) smoothing and gradient extraction (C) binarization and (D) filtering. Picture (A1) shows an enlargement of the droplet zone of picture (A), its noise filtering process (A2) and (A3) and the final droplet identification in (A4)

4. DROPLET GROWTH

4.1 Evaluation Strategy

Before we discuss the method to evaluate the droplet growth, it is necessary to explain the strategy we followed to take advantage of the holographic informations.

First, as a result of a dimensional analysis we see that for a given nozzle and a given fluid, the growth of subcooled spray droplets $\dot{R} = dR/dt$ with R as the droplet radius, injected into an environment formed by pure saturated vapour of the same substance as the droplets depends on the injected mass flow rate $\dot{M}$, the saturation pressure of the vapour $p_v = p_{sat}$, the geometry of the hollowed-cone liquid sheet (see Fig.2), the dropsize and velocity distributions, as well as the degree of subcooling $\Delta T = T_{sat} - T$ of the droplets.

M and p_v are experimental parameters, which can be freely selected and combined as shown in Table 1, the geometry of the liquid sheet and the size and velocity distributions are obtained from the holograms; they also inform if phenomena like coalescence or secondary atomization should be taken into account and, finally, the degree of subcooling, which is directly measured along the spray for each experiment, indicates the longitude of the spray along which the droplet growth takes place. A scheme of the spray flow is presented in Fig.2. Here, three different zones can be appreciated: a hollow-cone liquid sheet attached to the nozzle, a drop developing zone which is formed by liquid ligaments and droplet chains, and finally a zone where the droplets appear full developed. If axial symmetry is supposed, the temperature T at each point of the spray can be expressed as a function of the z-coordinate. Under this assumption, characteristic liquid temperatures are also defined in Fig.2. The complete holographic information, as well as the temperature measurements were summarized by Chávez (1991) in his Dissertation. In those temperature measurements Chávez reports values of ΔT close to zero at a distance $z = 96$ nozzle diameters (approx. 60 mm). At this condition the droplets arise to their maximum size.

With respect to the holograms, in order to have an idea of the view field observable on a holographic reconstruction, when an optimized optical set up is used for the reconstruction of holograms, the scheme of Fig.3 is presented. The grey circle represents a zone of about 50 mm in diameter where the reconstructed scene appears free of optical aberrations and suitable to be evaluated. The centre of the circle corresponds to the optical axis of the light beam, which reconstructs the holographic scene; it propagates perpendicular to the spray axis. In the middle of the grey circle, that is, around the optical axis, the scene appears very clear and almost free of optical noise. Therefore, we decided to situate the lower edge of the spray nozzle 5 mm upwards from the optical axis in order to reconstruct as clear as possible the liquid sheet zone, as well as the drop developing zone. So, if further holograms of the same spray, that is, at the same flow conditions are needed without loss of information at any section of the spray, the nozzle should be moved 50 mm upwards from its former position in the autoclave (see Fig.4) for the next hologram record.

Summarizing, the information from two holograms with optical axis at $z = 5$ mm and $z = 55$ mm is sufficient to evaluate the total droplet growth as shown in the next section.

4.2 Evaluation of the Droplet Growth

The holographic evaluation supplies, among other spacial information, the amount of droplets N (700 to 7000 droplets per hologram) distributed in Ni groups

$$N = \sum_{1}^{i} Ni \qquad (4)$$

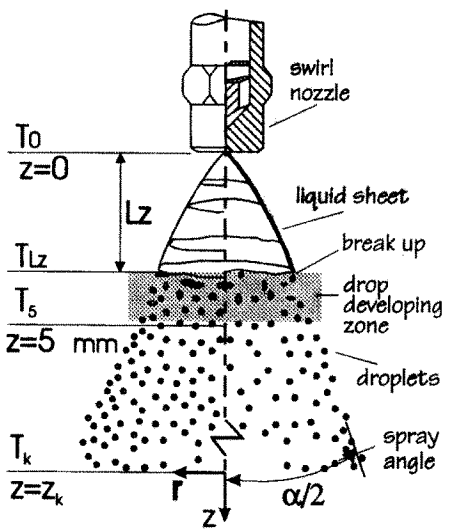

Fig. 2. Spray flow from a pressure swirl nozzle and temperature definitions

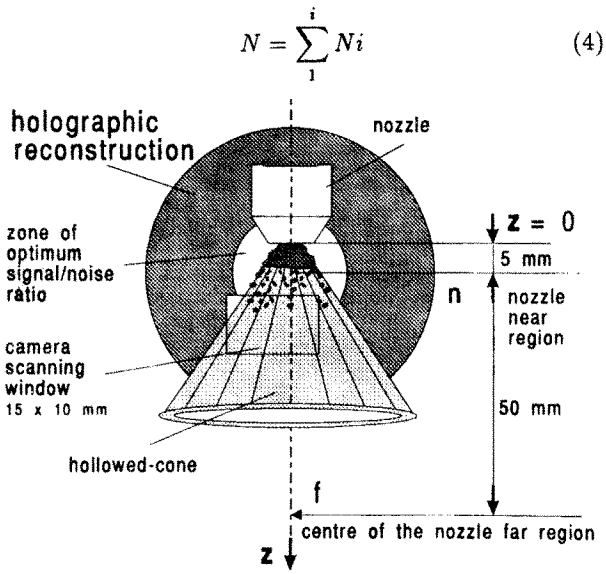

Fig. 3. View field in a holographic reconstruction

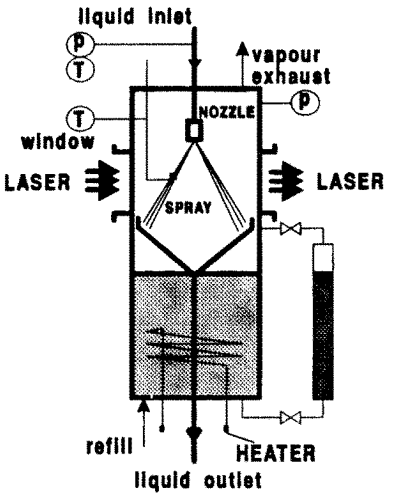

Fig. 4. Autoclave for experiments at controlled conditions of injection mass flow rate and vapour pressure. The nozzle can be moved vertically to allow for observation of any spray section

with i representing the subindex of the size class Di, the size class Di for which Ni arises to its maximum value N_{max}, the mean drop diameter

$$\bar{D} = \frac{\sum Ni\, Di}{\sum Ni}, \tag{5}$$

the Sauter mean diameter

$$D_{32} = \frac{\sum Ni\, Di^3}{\sum Ni\, Di^2} \tag{6}$$

the mean droplet velocity relative to the continuous phase around the droplets

$$\bar{U} = \frac{\sum Ni\, Ui}{\sum Ni}, \tag{7}$$

and the geometry of the liquid sheet represented by the mean discharge angle α_m and the break up length Lz at which the liquid sheet breaks up into liquid ligaments and drop chains (see Fig.2 for definitions).

Using this information, we can define a mean droplet growth $\delta\bar{D}$ calculated from the difference between the frequence distributions $N(D)_f$ and $N(D)_d$ in the nozzle far and near regions respectively. If this difference is normalized with N_{max} results

$$\delta D = \frac{N(D)}{N_{max}}|_f - \frac{N(D)}{N_{max}}|_d \tag{8}$$

which integral along the whole droplet size intervall D_{min} to D_{max} is

$$\frac{\delta D}{D} = \sum_{i_{min}}^{i_{max}} \frac{1}{Di}\left[\frac{\Delta D\, N(Di)}{N_{max}}|_f - \frac{\Delta D\, N(Di)}{N_{max}}|_d\right] \tag{9}$$

with ΔD meaning the interval between D_{i-1} and Di. Examples of this calculation as a function of Di are presented in the diagrams of Fig.5. Here $\frac{\delta D}{D}$ is presented in cumulative form $\sum \frac{\delta D}{D}$ to emphasize the tendence of the curves. The curves start at the negative side of the graphic or with negative slope due to a diminution of the population of small drops along the z-coordinate as a result of the condensation. By increasing Di, the curves change to positive slopes and finish at the positive side of the graphic, representing a net dropsize increase.

Finally, a mean droplet growth between the reference positions $z = 5$ mm and $z = 55$ mm can be obtained by multiplying $\frac{\delta D}{D}$ with the mean drop diameter $\bar{D}$

$$\delta\bar{D} = \frac{\delta D}{D}\,\bar{D} \tag{10}$$

which directly represents the intensity of the condensation and is related with the droplet growth $\dot{R}$ with the aid of Eq.(11)

$$\delta\bar{D} = 2\int \dot{R}\, dt. \tag{11}$$

In Eq.(11), the integral is performed for a time intervall during which the condensation of the vapour on the droplets causes an increase in dropsize equal to $\delta\bar{D}$. This

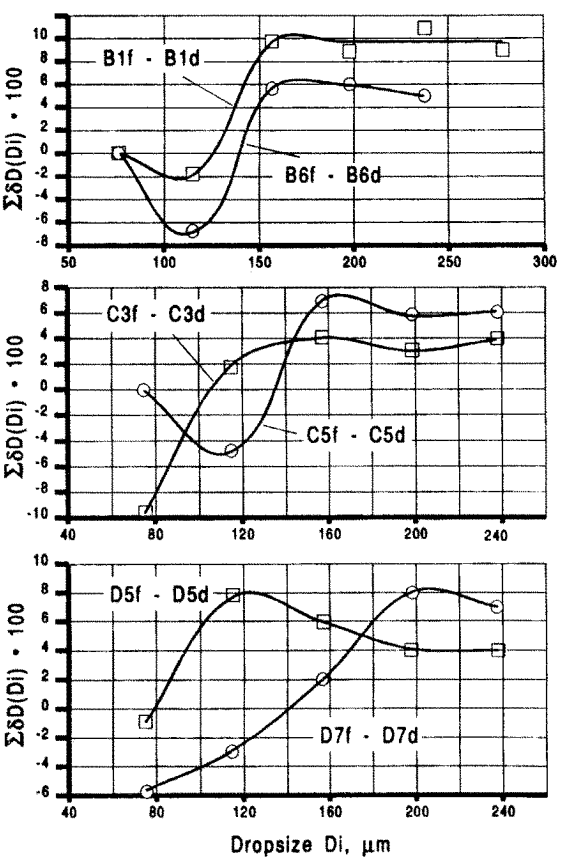

Fig. 5. Dropsize increment δD as a function of the dropsize class Di expressed in cumulative form

equation plays a very important role in the present evaluation method, because it relates a space-resolved quantity ($\delta\bar{D}$) with a time-resolved one ($\dot{R}$) and is the base of the condensation rate calculation.

5. HEAT TRANSFER COEFFICIENT

The application of Eq.(10) to the droplet distributions measured from the holograms could be enough to estimate the heat transfer coefficient h_D between the reference positions $z = 5$ mm and $z = 55$ mm, nevertheless in order to winn generality, the computation of h_D must be performed independently of these references. The problem in doing that appears because of the spray zone where the hollowed-cone liquid sheet breaks up but the originated droplets are not yet fully developed and, therefore, they cannot be measured. This zone extends from $z = Lz$ to approximately $z = 5$ mm. Based on the work by Chávez (1991) we propose the following procedure to obtain a general form of evaluating the heat transfer coefficient h_D.

5.1 Evaluation of the Condensation Rate

First, we considerate that at $z = z_k$ the droplet temperature T_k is equal to the saturation temperature T_{sat} and by assuming that for the time intervall at which the condensation takes place, all the liquid contained in the continuous hollowed-cone sheet breaks up into droplets of diameter equivalent to the Sauter mean diameter D_{32}, we arise to Eq.(12)

$$T_{sat} - T_5 = \frac{h_{fg}}{c_{p_l}} \frac{\varrho_l - \varrho_v}{\varrho_l} \frac{3\,\delta\bar{D}}{D_{32}} \tag{12}$$

from which T_5 (see Fig.2 for temperature definitions) can be calculated. In Eq.(12) h_{fg} means the enthalpy of evaporation and c_{p_l} the specific heat of the liquid. Further, by assuming ideal condensation at the liquid sheet we obtain Eq.(13)

$$T_{Lz} - T_0 = \frac{h_{fg}\,\dot{M}_S}{c_{p_l}\,\dot{M}} \tag{13}$$

where T_0 means the inlet temperature of the liquid measured at the nozzle outlet (at $z = 0$) as reported by Mayinger & Chávez (1992) and $\dot{M}_S$ represents the condensation rate at the liquid sheet. From this equation T_{Lz} can be known. Now, with T_5 and T_{Lz} an equivalent mean droplet growth $\delta\hat{D}$ for the droplet developing zone can be calculated as

$$\delta\hat{D} = \frac{c_{p_l}\,(T_5 - T_{Lz})\,D_{32}}{3\,h_{fg}} \tag{14}$$

with its help it is possible to evaluate the condensation rate $\dot{M}_D$ at the whole droplet collective, that is

$$\dot{M}_D = \frac{\varrho_l - \varrho_v}{\varrho_l} \frac{3(\delta\bar{D} + \delta\hat{D})}{D_{32}} (\dot{M} + \dot{M}_S) \tag{15}$$

which at arising the saturation conditions should be equivalent to

$$\dot{M}_D = \frac{c_{p_l}\,(\dot{M} + \dot{M}_S)\,(T_{sat} - T_{Lz})}{h_{fg}}. \tag{16}$$

This last equation permits to evaluate T_{Lz} again and after a couple of iterations, it is possible to find the real value of $\dot{M}_S$ without the necessity of assuming ideal condensation at the liquid sheet. Evaluations of $\dot{M}_D$ as a function of the mass flow rate $\dot{M}$ for different values of the vapour pressure p_v are presented in the diagram of Fig.6. Here we can observe a moderate dependence of $\dot{M}_D$ from $\dot{M}$ and a very strong dependence with respect to p_v. This behaviour results from the increase of p_v which also means an increase in the vapour density and, therefore, there is more vapour mass available for the condensation process.

5.2 Evaluation of the Heat Transfer Coefficient

The heat transfer coefficient h_D results from applying the condition of continuity of heat flux at the droplet surface (e.g. see Sundararayan & Ayyaswamy, 1984). In terms of the condensation rate $\dot{M}_D$, it can be expressed as

$$h_D = \frac{h_{fg}\,\dot{M}_D}{N_t\,\pi\,D_{32}^2\,(T_{sat} - T_{Lz})} \tag{17}$$

where N_t means the number of drops obtained as the quotient between the liquid volume contained in the liquid sheet and the volume of a mean droplet the diameter of which is equal to the Sauter mean diameter; in other words, N_t is a portion of N corresponding to the volume of the liquid sheet which is ideally followed until the droplets, initially at a temperature T_{Lz}, arise to their saturation temperature T_{sat}. From the holographic measurements of the break up lenght Lz and the mean spray angle α_m, N_t results

$$N_t = \frac{6\,\bar{\delta}_s\,L_z^2\,\mu\,\sin(\frac{\alpha_m}{2})}{D_{32}^3} \tag{18}$$

where $\bar{\delta}_s$ represents the mean thickness of the liquid sheet calculated by applying the condition of mass continuity at $z = Lz$ and with

$$\mu = \left[1 + \tan^2(\frac{\alpha_m}{2})\right]$$

resulting from the volume integration along the hollowed-cone (see Lee & Tankin, 1984 for details). The diagram of Fig.7 summarizes the measurements of the heat transfer coefficient α_D as a function of the mass flow rate $\dot{M}$ for different values of the vapour pressure p_v. At low values of the vapour pressure ($p_v < 0.4$ MPa), the influence of both $\dot{M}$ and p_v upon α_D is very strong and gradually decays at higher values of p_v. The reason of this behaviour bases on the diminution of the evaporation enthalpy

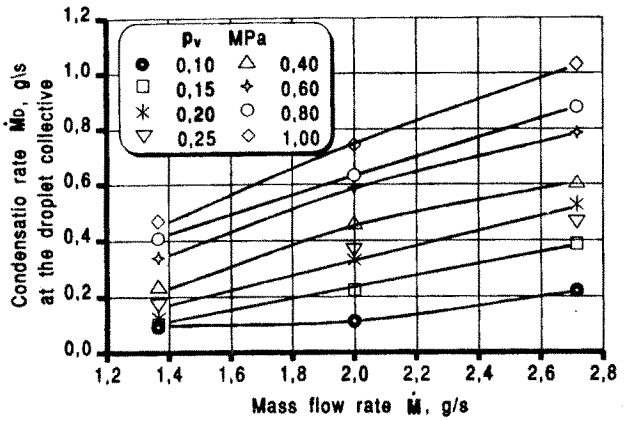

Fig. 6. Condensation rate $\dot{M}_D$ as a function of the mass flow rate $\dot{M}$ for different saturation pressures p_v

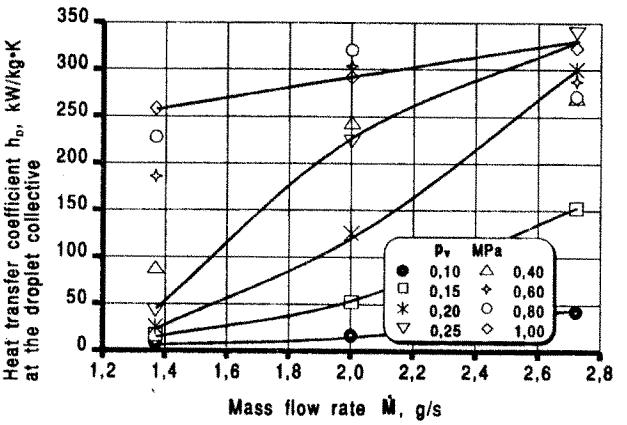

Fig. 7. Heat transfer coefficient h_D as a function of the mass flow rate $\dot{M}$ for different saturation pressures p_v

h_{fg} with p_v. Because of that, at higher values of p_v, the liquid looses slowly its ability to take energy from the vapour phase and in accordance with Eq.(17) α_D decrease in spite of the high values of $\dot{M}_D$.

6. UNCERTAINTY

There are two major error sources: the statistical error represented by the standard deviation of $\bar{D}$ and $\bar{U}$ which is of the order of 7% (Chávez, 1991) and the error in the measurements of the bulk liquid temperature along the spray. This error results inversely proportional to the subcooling ΔT. Chávez (1991) gives the variation intervall from 5% at $\Delta T > 20$ K to 30% at $\Delta \approx 1$ K.

Considering these error sources, the maximum relative error in the evaluation of the heat transfer coefficient, calculated through the logarithmic differentials of equations (8), (10), (12), (15) and (17) resulted in the range of 8% to 23%.

7. CONCLUSION

The present work demonstrated the ability of the holographic methods to measure the heat transfer coefficient at the phase interface between subcooled liquid droplets and their saturated vapour environment.

The method of computation of α_D showed also how is it possible to relate spacial resolved information with time resolved quantities.

Finally, the order of magnitude of the calculated heat transfer coefficient as a result of the direct-contact condensation suggests us to apply sprays more frequently in industrial cooling processes.

ACKNOWLEDGEMENT

The authors wish to thank the Deutsche Forschungsgemeinschaft (DFG) for the financial support for this study.

REFERENCES

Chávez A.A. & Mayinger, F. (1988), Single- and double pulsed holography for the characterization of sprays of refrigerant R113 inyected into its own saturated vapor, En: *Experimental Heat Transfer, Fluid Mechanics and Thermodynamics, Eds.: R.K. Shah, E.N. Ganic and K.T. Yang*, Elsevier, NY, pp. 848-854.

Chávez A.A. & Mayinger, F. (1989), Evaluation of pulsed laser holograms by applying digital image processing, *Proc. of the 9th Intl. Conference on Heat Transfer*, Jerusalem 19-24 Aug., Hemisphere, NY, pp. 187-192.

Chávez A.A. (1991), Holografische Untersuchung an Einspritzstrahlen –Fluiddynamik und Wärme Übergang durch Kondensation–, Dissertation, T.U. München.

Hasson, D., Luss, D. & Navon, U. (1964), An experimental study of steam condensation on a water sheet, *Int. J. Heat and Mass Tranfer*, Vol. 27, No. 7, pp. 983-1001.

Lautenschlager, G. (1988), Wärmeübergang in Krummern bei Sprühkühlung, Dissertation, T.U. München.

Lee, S.Y. & Tankin, R.S. (1984), Study of liquid spray (water) in a condensable environment (steam), *Int. J. Heat and Mass Tranfer*, Vol. 27, No. 3, pp. 363-374.

Mayinger, F. & Chávez, A.A. (1992), Measurement of direct-contact condensation of pure saturated vapour on an injection spray by applying pulsed laser holography, *Int. J. Heat and Mass Tranfer*, Vol. 35, No. 3, pp. 691-702.

Sideman, S. & Shabatai, H. (1964), Direct-contact heat transfer between a single drop and an inmiscible liquid medium, *The Can. J. of Chem. Engng.*, pp. 107-115.

Sundararayan, T. & Ayyaswamy, P.S. (1984), Hydrodynamics and heat transfer associated with condensation on a moving drop: Solutions for intermediate Reynolds numbers by a boundary layer formulation, *ASME, Journal of Heat Transfer*, Vol. 107, pp. 409-415.